SYSTEM IDENTIFICATION OF ABKOWITZ MODEL FOR SHIP MANEUVERING MOTION BASED ON ε-SUPPORT VECTOR REGRESSION

5 authors, including:

Bin Liu
Newcastle University
12 PUBLICATIONS **134** CITATIONS

SEE PROFILE

Allan R Magee
Technology Centre for Offshore and Marine, Singapore
99 PUBLICATIONS **609** CITATIONS

SEE PROFILE

OMAE2019-96699

SYSTEM IDENTIFICATION OF ABKOWITZ MODEL FOR SHIP MANEUVERING MOTION BASED ON ε-SUPPORT VECTOR REGRESSION

B. Liu[*]   **Y. Jin**   **A. R. Magee**[†]   **L. J. Yiew**   **S. Zhang**
Technology Centre for Offshore and Marine, Singapore
12 Prince George's Park, Singapore 118411
Singapore

ABSTRACT

System identification is crucial to predict the maneuverability of the ship. In this work, ε-support vector regression (ε-SVR) is implemented to identify hydrodynamic derivatives of Abkowitz maneuver model. A proposed technique, batch learning, is implemented with the addition of Gaussian white noise to reconstruct the samples and alleviate the parameter drift in the system identification of the ship maneuvering model. The predicted results are compared with results obtained from Planar Motion Mechanism (PMM) test. Standard maneuvers, $35°$ turning circle, $10°/10°$ and $20°/20°$ zigzags, are simulated and compared with the predicted model by ε-SVR. The presented results show that the proposed batch learning technique with Gaussian white noise is an effective technique, which improves the accuracy and robustness of ε-SVR in system identification. The results obtained from the predicted model match well with the those obtained from PMM results, which shows its excellent generalization performance. The developed model is applied to understand control requirements for vessels under different conditions.

Keywords: system identification, Abkowitz model, ε-support vector regression, parameter drift, batch learning

---

[*]Email: liu_bin@tcoms.sg
[†]Email: allan_magee@tcoms.sg

1 INTRODUCTION

The maritime industry is rapidly moving towards remotely controlled vessels, involving sensing, data-driven machine learning and autonomous maneuvering to enhance safety and alleviate the shortage of skilled seamen. For operations in open seas, the maneuverability of autonomous vessels in winds, waves and currents have to be better understood to develop more sophisticated digital twins to train on-board artificial intelligence (AI) control algorithms. To develop a strategy for autonomous vessels, the prediction of ship maneuverability is a critical procedure and required by the International Maritime Organization (IMO) [1] at the design stage of vessel.

System identification (SI) is an effective data-driven approach to predict the ship maneuverability, in which the hydrodynamic derivatives representing the intrinsic hydrodynamic features of a ship are identified. SI is used in engineering sciences to build mathematical models from data. Generally, there are two approaches to evaluate the ship maneuvering performances, experiments or simulations. In experimental methods, the data used for system identification is obtained from experiments, e.g., database, full-scale trials or free-running model tests. On the other hand, the data used for SI is obtained via mathematical model or computational fluid dynamics (CFD) simulations.

SI based on mathematical model is a popular and effective approach to predict the ship maneuverability. However, an accurate prediction also depends upon the the accuracy of the mathematical model representing the vessel. Commonly used ship maneuvering models are Abkowitz maneuver ship model [2], MMG

model [3] and response model [4]. Among aforementioned ship maneuvering models, Abkowitz and MMG models are often used in ship maneuvering community, because the available data provide a more comprehensive representation of the vessel maneuverability. In present investigation, we performed SI based on data generated from Abkowitz model.

To identify the governing mathematical model from collected data, many SI techniques have been proposed for nonlinear systems over the last decades, e.g., model reference method [5,6], extended Kalman filter [7,8], least squares [9,10], maximum likelihood [11], recursive prediction error [12], frequency spectrum analysis [13], particle swarm optimization [14], genetic algorithm [15], neural networks [16] and support vector machine (SVM) [17,18].

Nowadays, neural networks and machine learning techniques attract attention among research communities and exhibited their potentials in numerous applications. For example, the SVM is a very elegant algorithm among all kernel-learning methods. It is rooted in statistical learning theory, and provides an unique and optimal solution with a given data set [19]. Unlike recursive methods, e.g, artificial neural networks, it does not 'trap' into a local minimum and only converge to the global minimum. It is well-known for the 'kernel trick' in which the nonlinear data set is projected into higher dimensional feature space, where it may possibly become linear independent. This characteristics makes it very appealing to problems with strong nonlinearity and noise. Furthermore, many improvements in classical control design were achieved by integrating machine learning techniques [20–24]. In present investigation, an ε-SVR is applied to identify the hydrodynamic derivatives of the Abkowitz model. A batch learning technique is proposed to work together with Gaussian white noise to alleviate the parameter drift. The investigations are carried out for a series of maneuvering motion including a 35° turning circle, 10°/10° zigzag and 20°/20° zigzag maneuver. The identified maneuvering derivatives are compared with PMM measured data.

The remainder of the paper is organized as follows. The mathematical model of ship maneuver motion is described in Sect. 2. Subsequently, the formulation of ε-SVR and proposed batch learning are presented in Sect. 3. Following that, the methodology adopted in SI using ε-SVR is discussed in detail in Sect. 4. To alleviate the parameter drift issue in SI, a batch learning scheme is proposed in Sect. 5. The prediction results of hydrodynamic derivatives are discussed in Sect. 6. The comparison of the trajectories of Abkowitz models based on PMM results and predicted hydrodynamic derivatives are discussed in Sect. 7. Finally, concluding remarks are made in Sect. 8.

2 MATHEMATICAL MODEL OF SHIP MANEUVER MOTION

The dimensionless Abkowitz maneuver model in the perturbed form is presented in Eq. 1. This maneuvering model includes equations of surge, sway and yaw motions. Two coordinate systems are used in the simulation, the earth-fixed global inertial frame $o_0 - x_0 y_0 z_0$ and body-fixed local moving frame $o - xyz$. The body-fixed coordinate system is measured on the calm water free surface level, in which z_0-axis points downward. The x axis of body-fixed coordinate system is pointing at the forward of mid-ship. The x-y plane of two coordinate systems coincide. The respective axes of two coordinate systems, e.g., x axes, are parallel at the initial state.

$$\begin{bmatrix} m' - X'_{\dot{u}} & 0 & 0 \\ 0 & m' - Y'_{\dot{v}} & m'x'_G - Y'_{\dot{r}} \\ 0 & m'x'_G - N'_{\dot{v}} & I'_z - N'_{\dot{r}} \end{bmatrix} \begin{bmatrix} \Delta \dot{u}' \\ \Delta \dot{v}' \\ \Delta \dot{r}' \end{bmatrix} = \begin{bmatrix} \Delta F'_1 \\ \Delta F'_2 \\ \Delta F'_3 \end{bmatrix} \quad (1)$$

The prime denotes corresponding dimensionless quantities, which are defined as

$$m' = \frac{m}{\frac{1}{2}\rho L^3} \quad X'_{\dot{u}} = \frac{X_{\dot{u}}}{\frac{1}{2}\rho L^3} \quad Y'_{\dot{v}} = \frac{Y_{\dot{v}}}{\frac{1}{2}\rho L^3} \quad Y'_{\dot{r}} = \frac{Y_{\dot{r}}}{\frac{1}{2}\rho L^4}$$

$$N'_{\dot{v}} = \frac{N_{\dot{v}}}{\frac{1}{2}\rho L^4} \quad N'_{\dot{r}} = \frac{N_{\dot{r}}}{\frac{1}{2}\rho L^5} \quad I'_z = \frac{I_z}{\frac{1}{2}\rho L^5} \quad \Delta \dot{u}' = \frac{\Delta \dot{u}}{\frac{U^2}{L}}$$

$$\Delta \dot{v}' = \frac{\Delta \dot{v}}{\frac{U^2}{L}} \quad \Delta \dot{r}' = \frac{\Delta \dot{r}}{(\frac{U}{L})^2} \quad \Delta u' = \frac{\Delta u}{U} \quad \Delta v' = \frac{\Delta v}{U}$$

$$\Delta r' = \frac{L\Delta r}{U} \quad \Delta \delta' = \Delta \delta$$

where m, ρ, L and U are mass of ship, density of fluid, ship length and ship forward speed. u, v, $r = \dot{\psi}$, ψ and δ respectively are longitudinal velocity, transverse velocity, the yaw rate, yaw angle and rudder angle. The right-hand side terms are defined as

$$\Delta F'_1 = X'_u \Delta u' + X'_{uu} \Delta u'^2 + X'_{uuu} \Delta u'^3 + X'_{vv} \Delta v'^2 + X'_{rr} \Delta r'^2$$
$$+ X'_{vr} \Delta v' \Delta r + X'_{\delta\delta} \Delta \delta'^2 + X'_{\delta\delta u} \Delta \delta'^2 \Delta u'$$
$$+ X'_{v\delta} \Delta v' \Delta \delta' + X'_{v\delta u} \Delta v' \Delta \delta' \Delta u' \quad (2)$$

$$\Delta F'_2 = Y'_v \Delta v' + Y'_r \Delta r' + Y'_{vvv} \Delta v'^3 + Y'_{vvr} \Delta v'^2 \Delta r'$$
$$+ Y'_{vu} \Delta v' \Delta u' + Y'_{ru} \Delta r' \Delta u' + Y'_\delta \Delta \delta' + Y'_{\delta\delta\delta} \Delta \delta'^3$$
$$+ Y'_{\delta u} \Delta \delta' \Delta u' + Y'_{\delta uu} \Delta \delta' \Delta u'^2 + Y'_{v\delta\delta} \Delta v' \Delta \delta'^2$$
$$+ Y'_{vv\delta} \Delta v'^2 \Delta \delta' + Y'_0 + Y'_{0u} \Delta u' + Y'_{0uu} \Delta u'^2 \quad (3)$$

$$\Delta F'_3 = N'_v \Delta v' + N'_r \Delta r' + N'_{vvv} \Delta v'^3 + N'_{vvr} \Delta v'^2 \Delta r'$$
$$+ N'_{vu} \Delta v' \Delta u' + N'_{ru} \Delta r' \Delta u' + N'_\delta \Delta \delta' + N'_{\delta\delta\delta} \Delta \delta'^3$$
$$+ N'_{\delta u} \Delta \delta' \Delta u' + N'_{\delta uu} \Delta \delta' \Delta u'^2 + N'_{v\delta\delta} \Delta v' \Delta \delta'^2$$
$$+ N'_{vv\delta} \Delta v'^2 \Delta \delta' + N'_0 + N'_{0u} \Delta u' + N'_{0uu} \Delta u'^2 \quad (4)$$

where X_u', X_u', Y_v', Y_r', N_r', N_r' etc. are the dimensionless linear and nonlinear hydrodynamic derivatives. x_G and I_z refer to the longitudinal coordinate of the center of gravity of ship and the moment of inertia about z axis respectively. Y_0' and N_0' denote the dimensionless hydrodynamic forces in the y direction and the yaw moment about z axis during the steady forward motion at constant speed.

The state variables with subscript "0" refer to the states of vessel in the steady forward motion condition, e.g., $u_0 = U$ and $v_0 = r_0 = \delta_0 = \dot{u}_0 = \dot{v}_0 = \dot{r}_0 = 0$. The resultant speed in horizontal plane $U = \sqrt{(u_0 + \Delta u)^2 + v^2}$. The maximum rate of change of rudder angle is set at $5°/s$.

3 ε-SVR FORMULATION

The SVM is originally derived in statistical learning theory and applied in the area of pattern recognition. By introducing ε-insensitive loss function, SVM is applied in nonlinear regression estimation, SVR. In SVR, the objective is to define an optimal hyperplane, Eq. 5, contains as many data as possible within the insensitive region, based on prescribed parameters.

$$f(\boldsymbol{x}_j) = \boldsymbol{w}^T \cdot \boldsymbol{\phi}(\boldsymbol{x}_j) + b \quad (\boldsymbol{x}_j \in \mathbb{R}^M, \boldsymbol{\phi}(\boldsymbol{x}_j) \in \mathbb{R}^N, \boldsymbol{w} \in \mathbb{R}^N) \quad (5)$$

where $f(\boldsymbol{x})$, b and $\mathbb{R}^n$ respectively are the estimated scalar output, optimal bias of the system and Euclidean space of dimension n, e.g., $f(\boldsymbol{x}) \in \mathbb{R}^0$ and $b \in \mathbb{R}^0$. Here n refers to the dimension of input sample $\boldsymbol{x}$. $\boldsymbol{x}$ and $\boldsymbol{w}$ are vector input and optimal weight matrix of system respectively. $\boldsymbol{\phi}(\boldsymbol{x})$ is a linear or nonlinear function and refers to the high-dimensional feature space $\mathbb{R}^N$ ($N \gg M$), into where the original data $\boldsymbol{x}$ is projected. In the high-dimensional feature space, the original nonlinear data could be possibly linearized such that linear operations are applicable. The most attractive characteristics of SVM is that the coordinates in high-dimensional feature space is not explicitly required for computation.

In SVR, the regression problem is interpreted as an optimization problem subject to an objective function in primal formula, as shown in Eq. 6.

The optimization will minimize:

$$\boldsymbol{J}(\boldsymbol{w}, \xi_i, \xi_i^*) = \frac{1}{2}\boldsymbol{w}^T \cdot \boldsymbol{w} + C\sum_{i=1}^{N}(\xi_i + \xi_i^*) \quad (6)$$

subjected to

$$\begin{aligned} y_i - (\boldsymbol{w}^T \cdot \boldsymbol{\phi}(\boldsymbol{x}_i) + b) &\leq \varepsilon + \xi_i \quad &\forall i \\ (\boldsymbol{w}^T \cdot \boldsymbol{\phi}(\boldsymbol{x}_i) + b) - y_i &\leq \varepsilon + \xi_i^* \quad &\forall i \\ \xi_i, \xi_i^* &\geq 0 \quad &\forall i \end{aligned}$$

where y is the desired responses. ξ and ξ^* are slack variables, which define the upper limit of regression errors until which the constraints are still satisfied. ε is an insensitivity factor. It is introduced in an ε-insensitivity loss function, Eq. 7.

$$L_\varepsilon = \begin{cases} 0 & \text{if } |f(\boldsymbol{x}) - y| \leq \varepsilon \\ |f(\boldsymbol{x}) - y| - \varepsilon & \text{otherwise} \end{cases} \quad (7)$$

The parameter C is a regularization factor to prevent overfitting (regularization), which defines the trade-off between complexity of the machine to produce accurate results and the number of erroneous results, e.g, data outside ε margin.

Based on Karush-Kuhn-Tucker (KKT) conditions, this objective function in primal formula can be converted into a dual formula in Eq. 8, such that Eq. 8 is minimized

$$\begin{aligned} \boldsymbol{Q}(\alpha, \alpha^*) = &\frac{1}{2}\sum_{i=1}^{N}\sum_{j=1}^{N}(\alpha_i - \alpha_i^*)(\alpha_j - \alpha_j^*)\boldsymbol{\phi}^T(\boldsymbol{x}_i) \cdot \boldsymbol{\phi}(\boldsymbol{x}_j) \\ &+ \varepsilon\sum_{i=1}^{N}(\alpha_i + \alpha_i^*) - \sum_{i=1}^{N}y_i(\alpha_i - \alpha_i^*) \end{aligned} \quad (8)$$

subjected to

$$\begin{aligned} \sum_{i=1}^{N}(\alpha_i - \alpha_i^*) &= 0 \\ 0 \leq \alpha_i &\leq C \quad \forall i \\ 0 \leq \alpha_i^* &\leq C \quad \forall i \end{aligned}$$
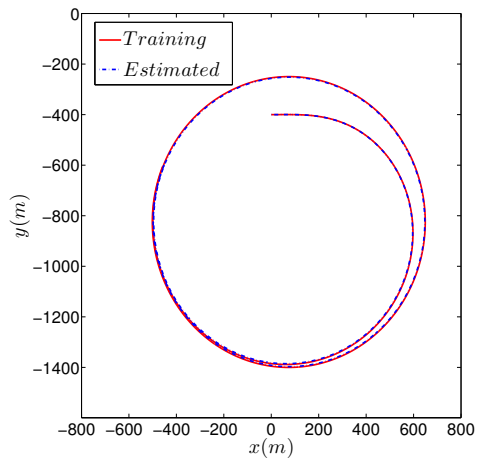
where α and α^* are Lagrange multipliers. By solving for α and α^*, the optimal hyperplane can be obtained by KKT conditions as

$$f(\boldsymbol{x}_j) = \sum_{i=1}^{N}(\alpha_i - \alpha_i^*)[\boldsymbol{\phi}^T(\boldsymbol{x}_i) \cdot \boldsymbol{\phi}(\boldsymbol{x}_j)] + b \quad (9)$$
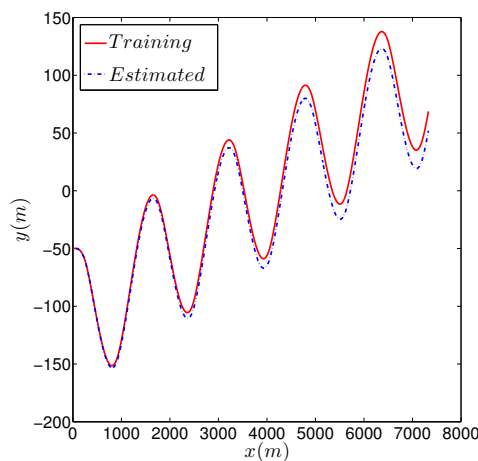
where N is the number of support vectors. If a linear kernel is used, one can obtain $\boldsymbol{w}$ and b as

$$\boldsymbol{w} = \sum_{i=1}^{N}(\alpha_i - \alpha_i^*)\boldsymbol{x}_i^T \quad (10)$$

$$b = y_j - \sum_{i=1}^{N}(\alpha_i - \alpha_i^*)\boldsymbol{x}_i^T \cdot \boldsymbol{x}_j - \varepsilon \cdot \text{sign}(\alpha_i - \alpha_i^*) \quad (11)$$

Copyright © 2019 ASME

(a)

(b)

FIGURE 1: Comparison of predicted motions with results from training simulation: (a) 35° turning circle; (b) 10°/10° zigzag

where $\overline{[\cdot]}$ and N refer to the mean value and total number of support vector. The optimal hyperplane becomes

$$f(\boldsymbol{x}_j) = \boldsymbol{w}^T \cdot \boldsymbol{x}_j + b \qquad (12)$$

4 METHODOLOGY

There are three sorts of SI approaches, the white-box (mechanism) modeling, the grey-box modeling and the black-box modeling. In white-box modeling, the mathematical model is known and reconstructed based on collected data. In the black-box modeling, only the collected input data is used to predict the maneuver motion, and no mathematical model is built. Whereas, the

Parameter	Value
Length overall (L_{oa})	171.8 (m)
Length between perpendiculars (L_{pp})	160.93 (m)
Maximum beam (B)	23.17 (m)
Design draft (T)	8.23 (m)
Design displacement (∇)	18541 (m^3)
Design speed (U_0)	15.5 (knots)
Maximum rudder rate (δ_{max})	$5°/s$
Dimensionless mass of ship (m')	7.98×10^{-3}
Dimensionless moment of inertia (I_z')	3.92×10^{-4}
Dimensionless longitudinal coordinate of ship's center of gravity (x_G')	-2.3×10^{-2}

TABLE 1: Main data parameters of Mariner class vessel

$\times 10^{-5}$	$X_{\dot{u}}'$	$Y_{\dot{v}}'$	$Y_{\dot{r}}'$	$N_{\dot{v}}'$	$N_{\dot{r}}'$
Value	-840	-1546	9	23	-83

TABLE 2: Predetermined hydrodynamic derivatives

grey-box modeling is used when the mathematical model is not fully known and reconstruction is not necessary. Since our objective to identify the linear and nonlinear hydrodynamic derivatives, the white-box modeling is used.

To estimate the hydrodynamic derivatives using ε-SVR, the Abkowitz model is re-cast into the following state-space form [18], as shown in Eq. 13a to 13c.

$$\boldsymbol{A}(k) \cdot \boldsymbol{X}^T = L(m' - X_{\dot{u}}')\dot{u}(k) \qquad (13a)$$

$$\boldsymbol{B}(k) \cdot \boldsymbol{Y}^T = L(m' - Y_{\dot{v}}')\dot{v}(k)$$
$$+ L^2(m'x_G' - Y_{\dot{r}}')\dot{r}(k) \qquad (13b)$$

$$\boldsymbol{C}(k) \cdot \boldsymbol{N}^T = L(m'x_G' - N_{\dot{v}}')\dot{v}(k)$$
$$+ L^2(I_z' - N_{\dot{r}}')\dot{r}(k) \qquad (13c)$$

where L is the ship length. The acceleration terms, e.g., $\dot{u}(k)$, $\dot{v}(k)$ and $\dot{r}(k)$ are approximated with Euler Forward scheme, as

$$\dot{u}(k) = \frac{\Delta u(k+1) - \Delta u(k)}{h} \qquad (14a)$$

$$\dot{v}(k) = \frac{v(k+1) - v(k)}{h} \qquad (14b)$$

$$\dot{r}(k) = \frac{r(k+1) - r(k)}{h} \qquad (14c)$$

4 Copyright © 2019 ASME

where h and k are the sampling interval and the time step index. The vectors X, Y and N are dimensionless hydrodynamic derivatives of surge, sway and yaw motions respectively, as shown in Eq. 15a to 15c.

$$X = [X'_u, X'_{uu}, X'_{uuu}, X'_{vv}, X'_{rr}, X'_{rv}, X'_{\delta\delta}, X'_{u\delta\delta}, X'_{v\delta},$$
$$X'_{uv\delta}] \tag{15a}$$
$$Y = [Y'_0, Y'_u, Y'_{uu}, Y'_v, Y'_r, Y'_{vvv}, Y'_{vvr}, Y'_{vu}, Y'_{ru}, Y'_\delta$$
$$Y'_{\delta\delta\delta}, Y'_{u\delta}, Y'_{uu\delta}, Y'_{v\delta\delta}, Y'_{vv\delta}] \tag{15b}$$
$$N = [N'_0, N'_u, N'_{uu}, N'_v, N'_r, N'_{vvv}, N'_{vvr}, N'_{vu}, N'_{ru}$$
$$N'_\delta, N'_{\delta\delta\delta}, N'_{u\delta}, N'_{uu\delta}, N'_{v\delta\delta}, N'_{vv\delta}] \tag{15c}$$

The corresponding dimensional state vectors are defined as

$$A(k) = \big[\Delta u(k)U(k), \Delta u^2(k), \frac{\Delta u^3(k)}{U(k)}, v^2(k), r^2(k)L^2,$$
$$v(k)r(k)L, \delta^2(k)U^2(k), \Delta u(k)\delta^2(k)U(k),$$
$$v(k)\delta(k)U(k), \Delta u(k)v(k)\delta(k)\big] \tag{16a}$$
$$B(k) = C(k) = \big[U^2(k), \Delta u(k)U(k), \Delta u^2(k), v(k)U(k),$$
$$r(k)U(k)L, \frac{v^3(k)}{U(k)}, \frac{v^2(k)r(k)L}{U(k)}, v(k)\Delta u(k),$$
$$r(k)\Delta u(k)L, \delta(k)U^2(k), \delta^3(k)U^2(k)$$
$$\Delta u(k)\delta(k)U(k), \Delta u^2(k)\delta(k), v(k)\delta^2(k)U(k),$$
$$v^2(k)\delta(k)\big] \tag{16b}$$

Recollecting Eq. 12 and Eq. 15a to Eq. 15c, one can notice that X, Y and N can be obtained by computing w at $b \approx 0$. In the next section, we will discuss a critical issue in the system identification of a strong nonlinear system, parameter drift.

5 PARAMETER DRIFT AND ε-SVR WITH BATCH LEARNING

Owing to the intrinsic nature of hydrodynamics of fluid, strong nonlinearity is common in maneuvering model, e.g., the X, Y and N terms in the Abkowitz model. This strong nonlinearity among hydrodynamic derivative terms can lead to a severe issue, parameter drift, in system identification of a maneuvering model [25]. In other words, the solution of hydrodynamic derivatives is not unique. When the parameter drift occurs, the obtained hydrodynamic derivatives could be wrong. These hydrodynamic derivatives maybe be correctly determined and able to reproduce the training maneuver, but fails to predict the other maneuvers of the same vessel.

Many authors [17, 18, 26] have successfully reduced the parameter drift by adding (zero-mean) Gaussian white noise into the sample data. The Gaussian white noise serves as a source

of perturbations to the maneuver parameters, e.g., rudder angle. Those perturbations make the maneuver parameter effective in the dynamics of vessel and identifiable by SVR. Recently new measures are proposed [25] to minimize the parameter drift, e.g, reconstruction of sample data and modification of the maneuver model. In present investigation, we propose an improvement to reduce the parameter drift further by combining Gaussian white noise and a batch learning scheme, in which we allow the ε-SVR to learn two different maneuvers of the same vessel. By learning two different maneuvers together, our objective is to reduce the linear dependency of training data matrix in the sample. The detailed modifications are shown below.

To train the SVR with the sample data, the samples at different time steps are projected into feature space with ϕ function and arranged into a matrix form, as shown in Eq. 17a to 17c.

$$A = [A(1), A(2), ..., A(l)]^T \tag{17a}$$
$$B = [B(1), B(2), ..., B(l)]^T \tag{17b}$$
$$C = [C(1), C(2), ..., C(l)]^T \tag{17c}$$

where l is the total number of sampling data in the time history. Parameter drift occurs due to the dynamic cancellation of linear hydrodynamic derivatives and multicolinearity of nonlinear hydrodynamic derivatives [25]. To alleviate the linear dependency between each column in matrices A, B and C respectively, sample data of two maneuvers are consolidated. Based on Eq. 13a to 13c, the Abkowitz model is re-cast as,

$$(A_1 + A_2) \cdot X^T = L(m' - X'_{\dot{u}})(\dot{u}_1 + \dot{u}_2) \tag{18a}$$
$$(B_1 + B_2) \cdot Y^T = L(m' - Y'_{\dot{v}})(\dot{v}_1 + \dot{v}_2)$$
$$+ L^2(m'x'_G - Y'_{\dot{r}})(\dot{r}_1 + \dot{r}_2) \tag{18b}$$
$$(C_1 + C_2) \cdot N^T = L(m'x'_G - N'_{\dot{v}})(\dot{v}_1 + \dot{v}_2)$$
$$+ L^2(I'_z - N'_{\dot{r}})(\dot{r}_1 + \dot{r}_2) \tag{18c}$$

where subscript "1" and "2" refer to different maneuvers. Here we assume that hydrodynamic derivatives X, Y and N are constant among different maneuvers. Ideally, the more different two maneuvers are, e.g., turning circle and zigzag, the wider variations of speeds, drift angle, rudder angles and rotation rates are. As a result, the linear dependency between columns in $A_1 + A_2$, $B_1 + B_2$ and $C_1 + C_2$ are reduced. In the next section, the performance of proposed batch learning together with addition of Gaussian white noise is evaluated by comparison with PMM and literature results.

6 PREDICTED RESULTS

To evaluate the performance of the proposed ε-SVR with batch learning, a mariner class vessel [27] is taken as an example.

Copyright © 2019 ASME

Tab. 1 shows the main particulars of this vessel, in which L_{pp}, U_0, σ_{max}, m', I_z' and x_G' are used for simulation and prediction. The predetermined dimensionless hydrodynamic derivatives are summarized in Tab. 2.

The $35°$ turning circle and $10°/10°$ zigzag maneuvers are simulated for training of ε-SVR with batch learning. The hydrodynamic derivatives taken from PMM results [27] for simulation are summarized in Tab. 3, 4 and 5. The surge speed u, the sway speed v, the yaw rate r, the heading angle φ and the resultant speed U are collected based on the simulations. The simulation sampling interval is 1 s, and 400 samples are collected for training of ε-SVR. In SVM/SVR, we would like to achieve two things, correct classification/regression (high accuracy, low value of ε) and large margin (good generalization, low value of C). However, most of the time, we cannot achieve both. In our case, we aim at obtaining an excellent accuracy. Therefore, we choose a very low ε value, 1×10^{-16} and very high C value 1×10^6.

Two configurations are taken into consideration in Tab. 3, 4 and 5, (1) training with Gaussian white noise (G); (2) training with Gaussian white noise and proposed batching learning (G+B). The obtained results are compared with literature and PMM results, as summarized in Tab. 3, 4 and 5. The discrepancies with the PMM results are shown with percentage in parentheses.

It can be observed that the prediction of hydrodynamic derivatives for surge motion $\boldsymbol{X}$ is very stable and accurate among different methods in Tab. 3. On the other hand, the discrepancies between predicted results and PMM results are prominent. It is noteworthy that our results trained with only Gaussian white noise fails at the same hydrodynamic derivatives of sway and yaw motions to Wang et al. (2015) [18]. It is reasonable, since we applied a similar technique. However, because the results are sensitive to the magnitude of Gaussian white noise, training maneuver and temporal integration scheme, the level of discrepancies is different. The applied forward Euler temporal integration scheme can introduce large numerical errors at a relative large time step, which takes the similar role to the Gaussian white noise. Therefore, we presented the most accurate predictions with Gaussian white noise (Present (G)) at different settings, e.g., time step, sampling rate, sample size and noise level. We subsequently use these results to compare with the results obtained from the proposed batching scheme together with Gaussian white noise.

When Gaussian white noise and proposed batch learning scheme are used together to train ε-SVR (Present (G+B)), the improvement in accuracy and robustness of prediction of hydrodynamic derivatives are significant. In total, there are 7 hydrodynamic derivatives which are different from PMM results, compared with prediction with Gaussian white noise, where at least 24 erroneous hydrodynamic derivatives are observed, as shown in Tab. 3, 4 and 5. The accuracy is generally controlled around 1%, except one hydrodynamic derivative $N_{v\delta\delta}'$. Furthermore, the

results presented for batch learning are randomly chosen, instead of the best among the available results. The accuracy and robustness of proposed batch learning with Gaussian white noise remains good within a relatively wide range of parametric space, e.g., sampling rate, sample size, different maneuvers and noise level.

7 DISCUSSION OF VERIFICATION RESULTS

In this section, the trajectories of different maneuvers based on PMM results and estimated hydrodynamic derivatives are compared. The objective is to evaluate the generalization of the mathematical model based on estimated hydrodynamic derivatives in Tab. 3, 4 and 5.

The comparisons of vessel's motion between the predicted motions and the results from training simulation are shown in Fig. 1. In Fig. 1a, the rudder is turned $35°$. The predicted motion matches very well with the training result. On the other hand, the small discrepancy between the predicted motion and training results of $10°/10°$ zigzag in Fig. 1b starts growing as time goes on. Although the predicted hydrodynamic derivatives using ε-SVR with batch learning are very close to PMM results, the accumulation of errors in long-time simulation is inevitable.

The comparisons between the predicted motions and the results from test simulations, $10°$ turning circle and $20°/20°$ zigzag are also conducted, as shown in Fig. 2 and 3. The sampling rate of test simulations is identical to training simulations. These comparisons show that the proposed ε-SVR with batching learning is robust and possess good generalization performance. It is capable of predicting the underlining Abkowitz maneuver model to reproduce simulated results.

8 CONCLUSION REMARK

In present investigation, An ε-SVR with batch learning was proposed to identify the hydrodynamic derivatives of an Abkowitz model, based on numerical results from simulations. It shown that the implemented system identification technique possesses following characteristics: (a) excellent accuracy in prediction of hydrodynamic derivatives; (b) reduce the number of erroneous hydrodynamic derivatives compared with PMM results; (c) an effective complementary technique together with the addition of Gaussian white noise to alleviate the parameter drift; (d) excellent generalization performance through learning multiple maneuvers simultaneously.
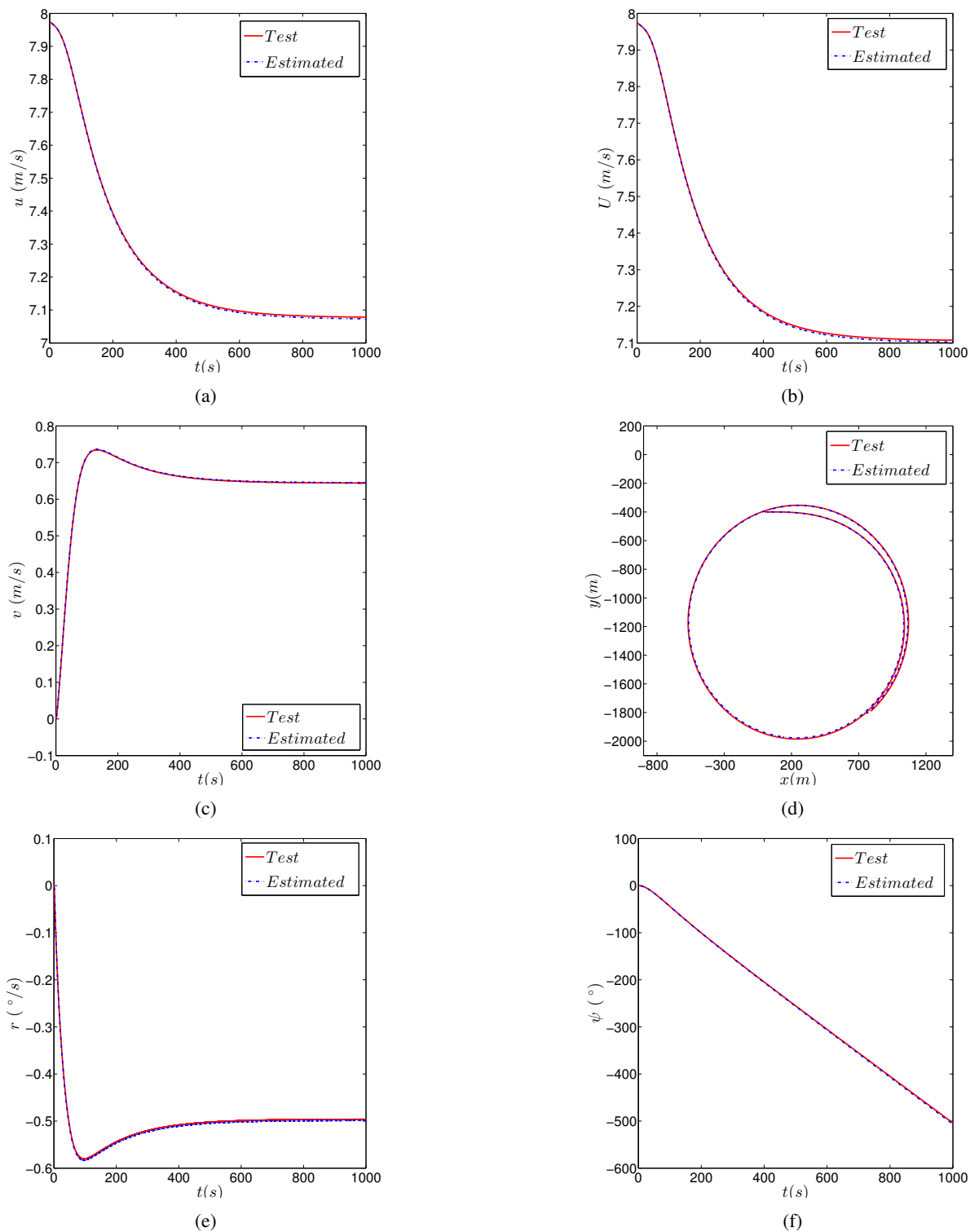
FIGURE 2: Comparison of predicted motions with results from test simulation, $10°$ turning circle: (a) u vs. t; (b) U vs. t; (c) v vs. t; (d) x vs. y; (e) r vs. t; (f) ψ vs. t
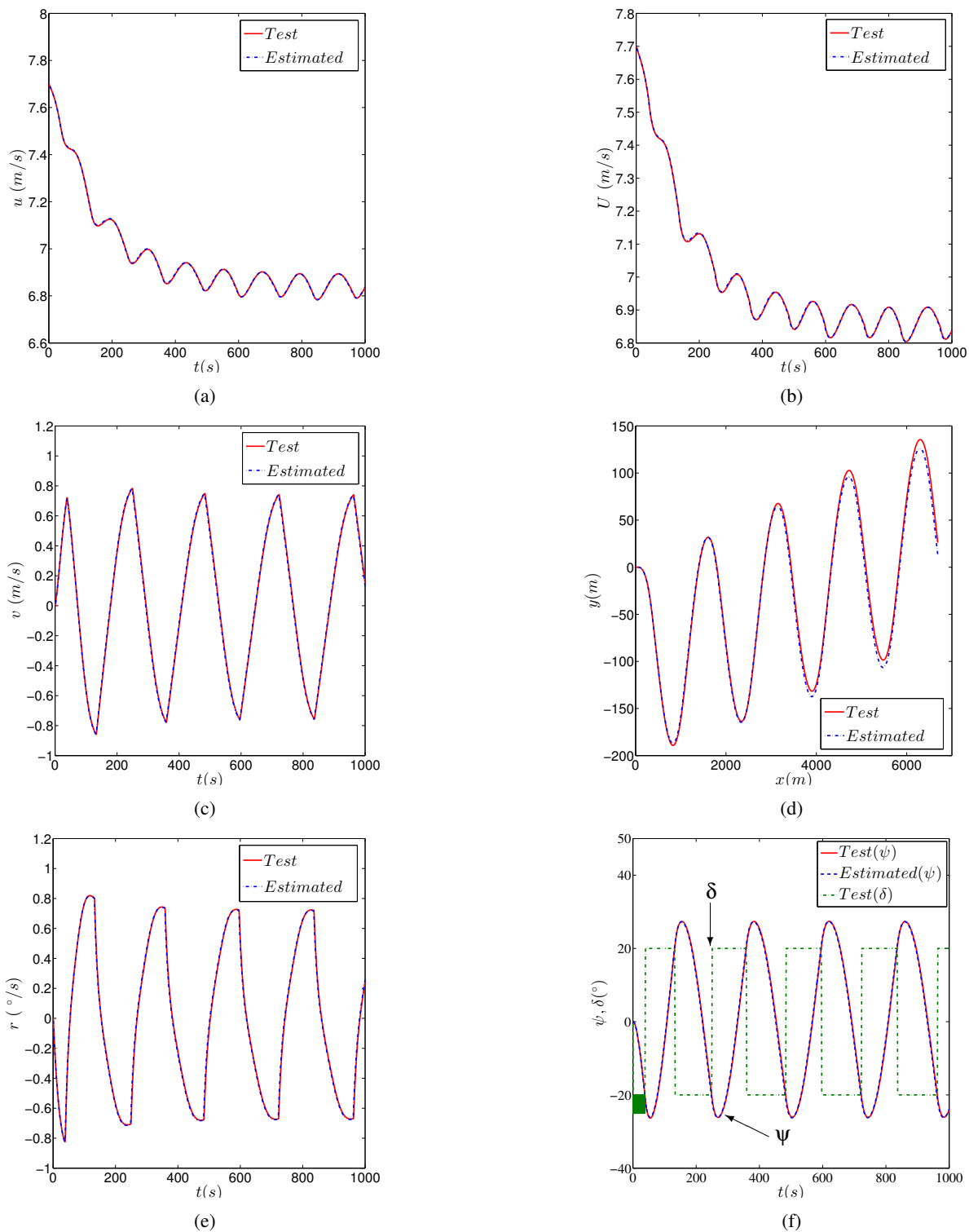
Copyright © 2019 ASME

FIGURE 3: Comparison of predicted motions with results from test simulation, $20°/20°$ zigzag: (a) u vs. t; (b) U vs. t; (c) v vs. t; (d) x vs. y; (e) r vs. t; (f) ψ vs. t

8

$\times 10^{-5}$	X_u'	X_{uu}'	X_{uuu}'	X_{vv}'	X_{rr}'	$X_{\delta\delta}'$	$X_{\delta\delta u}'$	X_{vr}'	$X_{v\delta}'$	$X_{v\delta u}'$
PMM [27]	-184	-110	-215	-899	18	-95	-190	798	93	93
Wang et al.(2015) [18]	-184	-111 (0.9%)	-217 (0.9%)	-900 (0.1%)	18	-95	-190	798	93	93
Present (G)	-184	-110	-215	-899	18	-95	-190	798	93	93
Present (G+B)	-184	-110	-215	-899	18	-95	-190	798	93	93

TABLE 3: Dimensionless hydrodynamic derivatives of surge motion: G and G+B respectively denote Gaussian white noise and Gaussian white noise with batch learning

$\times 10^{-5}$	Y_v'	Y_r'	Y_{vvv}'	Y_{vvr}'	Y_{vu}'	Y_{ru}'	Y_δ'	$Y_{\delta\delta\delta}'$	$Y_{u\delta}'$
PMM [27]	-1160	-499	-8078	15356	-1160	-499	278	-90	556
Wang et al.(2015) [18]	-1160	-499	-7950 (1.6%)	15413 (0.04%)	1133 (2.3%)	-485 (2.8%)	278	-93 (3.3%)	562 (1.1%)
Present (G)	-1160	-499	-8076 (0.03%)	15361 (0.03%)	-1143 (1.5%)	-494 (1%)	278	-90	557 (0.2%)
Present (G+B)	-1160	-499	-8080 (0.03%)	15354 (0.01%)	-1160	-499	278	-90	556

$\times 10^{-5}$	$Y_{uu\delta}'$	$Y_{v\delta\delta}'$	$Y_{vv\delta}'$	Y_0'	Y_{0u}'	Y_{0uu}'
PMM [27]	278	-4	1190	-4	-8	-4
Wang et al.(2015) [18]	294 (5.8%)	-3 (25%)	1209 (1.6%)	-3 (25%)	-10 (25%)	-5 (25%)
Present (G)	280 (0.7%)	-5 (25%)	1198 (0.7%)	-6 (50%)	-6 (25%)	-12 (200%)
Present (G+B)	279 (0.4%)	-4	1188 (0.2%)	-4	-8	-4

TABLE 4: Dimensionless hydrodynamic derivatives of sway motion: G and G+B respectively denote Gaussian white noise and Gaussian white noise with batch learning

REFERENCES

[1] IMO, 2002. "Standards for ship manoeuvrability". *Resol. MSC International Maritime Organization (IMO), 137*(76).

[2] Abkowitz, M. A., 1964. Lectures on ship hydrodynamics– steering and manoeuvrability. Tech. rep.

[3] Ogawa, A., and Kasai, H., 1978. "On the mathematical model of manoeuvring motion of ships". *International Shipbuilding Progress, 25*(292), pp. 306–319.

[4] Nomoto, K., Taguchi, T., Honda, K., and Hirano, S., 1957. "On the steering qualities of ships". *International Shipbuilding Progress, 4*(35), pp. 354–370.

[5] Hayes, M. N., 1971. "Parametric identification of nonlinear stochastic systems applied to ocean vehicle dynamics.".

[6] Van Amerongen, J., 1984. "Adaptive steering of ships: A model reference approach". *Automatica, 20*(1), pp. 3–14.

[7] Abkowitz, M. A., 1980. Measurement of hydrodynamic characteristics from ship maneuvering trials by system identification. Tech. rep.

[8] Perera, L. P., Oliveira, P., and Soares, C. G., 2015. "Sys-

$\times 10^{-5}$	N'_v	N'_r	N'_{vvv}	N'_{vvr}	N'_{vu}	N'_{ru}	N'_δ	$N'_{\delta\delta\delta}$	$N'_{u\delta}$
PMM [27]	-264	-166	-1636	-5483	-264	-166	-139	45	-278
Wang et al.(2015) [18]	-265 (0.4%)	-166	-1555 (5%)	-5529 (0.8%)	-284 (7.6%)	-176 (6%)	-139	45	-282 (1.4%)
Present (G)	-265 (0.4%)	-166	-1630 (0.4%)	-5481 (0.04%)	-263 (0.4%)	-167 (0.6%)	-139	45	-279 (0.4%)
Present (G+B)	-264	-166	-1632 (0.3%)	-5488 (0.09%)	-264	-166	-139	45	-278

$\times 10^{-5}$	$N'_{uu\delta}$	$N'_{v\delta\delta}$	$N'_{vv\delta}$	N'_0	N'_{0u}	N'_{0uu}
PMM [27]	-139	13	-489	3	6	3
Wang et al.(2015) [18]	-149 (7.2%)	13	-510 (4.3%)	2 (33.3%)	7 (16.7%)	2 (33.3%)
Present (G)	-141 (1.4%)	14 (7.7%)	-498 (1.8%)	14 (366.7%)	17 (183.3%)	16 (433.3%)
Present (G+B)	-139	14 (7.7%)	-489	3	6	3

TABLE 5: Dimensionless hydrodynamic derivatives of yaw motion: G and G+B respectively denote Gaussian white noise and Gaussian white noise with batch learning

tem identification of nonlinear vessel steering". *Journal of Offshore Mechanics and Arctic Engineering, 137*(3), p. 031302.

[9] Holzhüter, T., 1990. "Robust identification scheme in an adaptive track-controller for ships". In *Adaptive Systems in Control and Signal Processing 1989*. Elsevier, pp. 461–466.

[10] Muñoz-Mansilla, R., Aranda, J., Díaz, J. M., and De La Cruz, J., 2009. "Parametric model identification of high-speed craft dynamics". *Ocean Engineering, 36*(12-13), pp. 1025–1038.

[11] Astrom, K., 1979. "Maximum likelihood and prediction error methods". *IFAC Proceedings Volumes, 12*(8), pp. 551–574.

[12] Zhou, W.-W., and Blanke, M., 1989. "Identification of a class of nonlinear state-space models using rpe techniques". *IEEE Transactions on Automatic Control, 34*(3), pp. 312–316.

[13] Bhattacharyya, S., and Haddara, M., 2006. "Parametric identification for nonlinear ship maneuvering". *Journal of ship research, 50*(3), pp. 197–207.

[14] Chen, Y., Song, Y., and Chen, M., 2010. "Parameters identification for ship motion model based on particle swarm optimization". *Kybernetes, 39*(6), pp. 871–880.

[15] Sutulo, S., and Soares, C. G., 2014. "An algorithm for of-fline identification of ship manoeuvring mathematical models from free-running tests". *Ocean Engineering, 79*, pp. 10–25.

[16] Luo, W., and Zhang, Z., 2016. "Modeling of ship maneuvering motion using neural networks". *Journal of Marine Science and Application, 15*(4), pp. 426–432.

[17] Zhang, X.-g., and Zou, Z.-j., 2011. "Identification of abkowitz model for ship manoeuvring motion using ε-support vector regression". *Journal of hydrodynamics, 23*(3), pp. 353–360.

[18] Wang, X.-g., Zou, Z.-j., Hou, X.-r., and Xu, F., 2015. "System identification modelling of ship manoeuvring motion based on ε-support vector regression". *Journal of Hydrodynamics, 27*(4), pp. 502–512.

[19] Vapnik, V., 2013. *The nature of statistical learning theory*. Springer science & business media.

[20] Suykens, J. A., Vandewalle, J., and De Moor, B., 2001. "Optimal control by least squares support vector machines". *Neural networks, 14*(1), pp. 23–35.

[21] Ding, L. H. L., 2008. "Self-tuning pid controller for a nonlinear system based on support vector machines [j]". *Control Theory & Applications, 3*, p. 015.

[22] Zhang, L., Xi, Y.-G., and Zhou, W.-D., 2009. "Identification and control of discrete-time nonlinear systems using affine support vector machines". *International Journal on

Artificial Intelligence Tools, **18**(06), pp. 929–947.

[23] Iplikci, S., 2010. "A support vector machine based control application to the experimental three-tank system". *ISA transactions,* **49**(3), pp. 376–386.

[24] Abdessemed, F., 2012. "Svm-based control system for a robot manipulator". *International Journal of Advanced Robotic Systems,* **9**(6), p. 247.

[25] Luo, W., and Li, X., 2017. "Measures to diminish the parameter drift in the modeling of ship manoeuvring using system identification". *Applied Ocean Research,* **67**, pp. 9–20.

[26] Luo, W., and Zou, Z., 2009. "Parametric identification of ship maneuvering models by using support vector machines". *Journal of Ship Research,* **53**(1), pp. 19–30.

[27] Fossen, T. I., 2011. *Handbook of marine craft hydrodynamics and motion control.* John Wiley & Sons.

Copyright © 2019 ASME